

# Detecting Road Surface Wetness from Audio: A Deep Learning Approach

Irman Abdic<sup>12</sup>, Lex Fridman<sup>1</sup>, Erik Marchi<sup>2</sup>, Daniel Brown<sup>1</sup>, William Angell<sup>1</sup>, and Bryan Reimer<sup>1</sup>

<sup>1</sup>Massachusetts Institute of Technology (MIT)

<sup>2</sup>Technische Universität München (TUM)

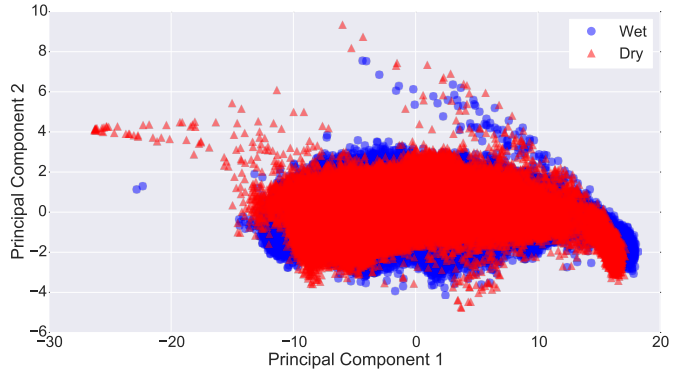
**Abstract**—We introduce a recurrent neural network architecture for automated road surface wetness detection from audio of tire-surface interaction. The robustness of our approach is evaluated on 785,826 bins of audio that span an extensive range of vehicle speeds, noises from the environment, road surface types, and pavement conditions including international roughness index (IRI) values from 25 in/mi to 1400 in/mi. The training and evaluation of the model are performed on different roads to minimize the impact of environmental and other external factors on the accuracy of the classification. We achieve an unweighted average recall (UAR) of 93.2% across all vehicle speeds including 0 mph. The classifier still works at 0 mph because the discriminating signal is present in the sound of other vehicles driving by. Removing audio segments at speeds below 2.9 mph from consideration improves the UAR to 100%. In the case when the vehicle speed is below 2.9 mph, we were able to discriminate between wet and dry road surfaces from ambient noises and achieve 74.5% UAR.

**Index Terms**—Road surface audio analysis; wetness detection; deep learning; safety systems; on-road driving data; LSTM; RNN.

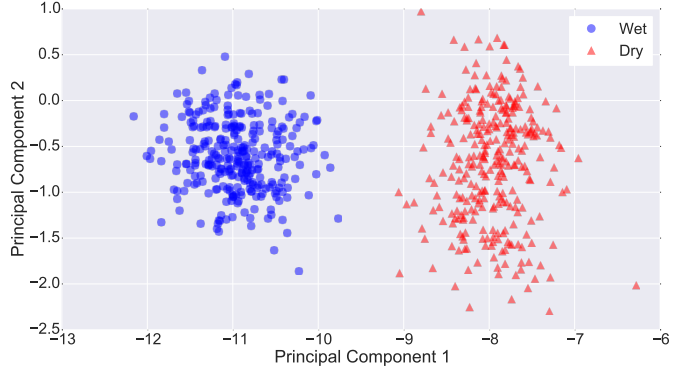
## I. INTRODUCTION

Wet pavement is responsible for 74% of all weather-related crashes in U.S. with over 380,000 injuries and 4,700 deaths per year [1]. Furthermore, wet roads often increase traffic congestion and result in infrastructure damage and supply chain disruptions [2]. From the perspective of driver safety, wetness detection during the period of time after the precipitation has ended but the road is still wet is critical. Under this conditions, human estimation of road wetness and friction properties is less accurate than normal, especially in reduced visibility over night or in the presence of fog [3].

The automated detection of road conditions from audio may be an important component of next generation Advanced Driver Assistance Systems (ADAS) that have the potential to enhance driver safety [4]. Moreover, autonomous and semi-autonomous vehicles have to be aware of road conditions to automatically adapt vehicle speed while entering the curve or keep a safe distance to the vehicle in front. There are numerous approaches that can detect whether a surface is wet or dry, but in the majority of cases they are not robust to variation in real-world datasets. Accuracy of video-based wetness prediction decreases significantly in poor lighting conditions (i.e., night,



(a) PCA for full wet 2 and dry 2 trips from Table I.



(b) PCA for a randomly-selected segment of road from wet 2 and dry 2 trips from Table I.

Fig. 1: PCA analysis for wet and dry road surfaces that illustrates a representative case where audio-based wetness detection is linearly separable for similar road type and vehicle speeds.

fog, smoke). Audio-based wetness prediction is heavily dependent upon surface type and vehicle speed which is fairly represented in our dataset of 785,826 bins (feature vectors described in §III-B) [5]. We elucidate this dependence by visualizing the first 2 principal components for (1) two full trips and (2) a small 10-second section of road from (1). These two visualizations are shown in Fig. 1a and Fig. 1b, respectively. The feature set we use is linearly separable for a specific road type and vehicle speed, as visualized in Fig. 1b.

However, given the nonlinear relation of our feature set for (1) that is visualized in Fig. 1a we applied Recurrent Neural Networks (RNNs) which can model and separate the data points.

## II. RELATED WORK

The long short-term memory RNNs (LSTM-RNN) have been successfully applied in many fields from hand writing recognition to robotic heart surgery [6], [7]. In the audio context, LSTM-RNN contributed to the development of better phoneme classification, emotion detection from speech, animal species identification and finding temporal structure in music [8]–[11]. However, in our best knowledge LSTM-RNN have not been applied to the task of road wetness detection.

Related works can be found in the video processing domain, where wetness detection has been studied with two camera set-ups: (1) a surveillance camera at night, and (2) a camera on-board a vehicle. The detection of road surface wetness using surveillance camera images at night is relying on passing cars' headlights as a lighting source that creates a reflection artifact on the road area [12]. On-board video cameras use polarization changes of reflections on road surfaces or spatio-temporal reflection models [13]–[15]. The drawback of both methods is the fact that they require (1) an external light source to be present and (2) visibility conditions to be clear.

Another approach capable of detecting road wetness relies on 24-GHz automotive radar technology for detecting low-friction spots [16]. It analyzes backscattering properties of wet, dry, and icy asphalt in laboratory and field experiments.

Traditionally, audio analysis of the road-tire interaction has been done by examining tire noises of passing vehicles from a stationary microphone positioned on the side of the road. This kind of analysis reveals that tire speed, vertical tire load, inflation pressure and driving torque are primary contributors to tire sound in dry road conditions [17]. Other on-road audio collecting devices for surface analysis can be found in specialized vehicles for pavement quality evaluation (e.g., VOTERS [18]) and for vehicles instrumented for studying driver behavior in the context of automation (e.g., MIT RIDER [19]). Finally, road wetness has been studied from on-board audio of tire-surface interaction, where SVMs have been applied [5].

The method described in our paper improves the prediction accuracy of this prior work and expands the evaluation to a wide range of surface types and pavement conditions. This is the first study that applies LSTM-RNN in this field. In addition, we improve on the following three aspects of [5] where (1) the model was trained and tested on the same road segment, (2) false predictions caused by the impact of pebbles on the vehicle chassis were ignored, and (3) audio segments associated with speeds below 18.6 mph were removed.

We trained and tested the model on different routes, and considered all predictions regardless of the speed, pebbles impact or any other factor.

## III. ROAD SURFACE WETNESS CLASSIFICATION

### A. Data Collection

For data collection purposes, we instrumented a 2014 Mercedes CLA with an inexpensive shotgun microphone behind the rear tire, as shown in Fig. 2. The gain level of the microphone and its distance from the tire were kept the same for the entire data collection process. Three different routes were selected. For each route, we drove the same exact path once during the rain (or immediately after) and another time when the road surface was completely dry, as shown in Fig. 3. The duration and length of trips ranged from 14 min to 30 min and 6.1 mi to 9.0 mi, respectively. The summary of the dataset is presented in Table I.



Fig. 2: Instrumented MIT AgeLab vehicle (left) and placement of the shotgun microphone behind the rear tire (right).



Fig. 3: Snapshots from the video of the forward roadway showing the same GPS location for a “wet” trip (left) and a “dry” trip (right). A video of these trips is available at: <http://lexfridman.com/wetroad>.

Trip	Time	Distance	Avg Speed	Avg IRI
wet 1	26min	9.0mi	7.4mph	267in/mi
wet 2	16min	6.4mi	9.4mph	189in/mi
wet 3	14min	6.1mi	13.5mph	142in/mi
dry 1	30min	9.0mi	9.6mph	267in/mi
dry 2	14min	6.4mi	9.1mph	189in/mi
dry 3	18min	6.1mi	9.3mph	142in/mi

TABLE I: Statistics of the collected data for six trips: time, distance, average speed and average IRI.

The data collection was carried out in Cambridge and the Greater Boston area with different speeds, traffic conditions and pavement roughness. The latter is measured with the International Roughness Index (IRI) which represents pavement

quality [20]. A histogram of IRI values for the collected dataset is presented in Fig. 4, wherein the unit of measurement is in inches per mile (in/mi). Our dataset contains values from 25 in/mi to 1400 in/mi, but in Fig. 4, values over 400 in/mi are aggregated into a single bin. According to the Massachusetts Department of Transportation (MassDOT) Road Inventory, the route we traveled is a combination of Surface-treated road and Bituminous concrete road [21].

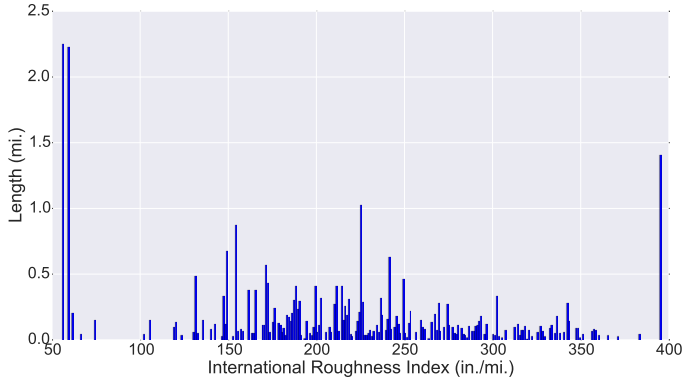


Fig. 4: Histogram of IRI distribution throughout collected data.

### B. Features

Our aim was to model the whole spectrum along with the first order differences and then select a subset of features that discriminates our classes the best. We extracted Auditory Spectral Features (ASF), that were computed by applying the short-time Fourier transform (STFT) using a frame size 30ms and a frame step of 10ms. Furthermore, each STFT power spectrogram has been converted to the Mel-Frequency scale using 26 triangular filters obtaining the Mel spectrograms  $M_{30}(n, m)$ . To match the human perception of loudness, a logarithmic representation has been chosen:

$$M_{log}^{30}(n, m) = \log(M_{30}(n, m) + 1.0) \quad (1)$$

In addition, the positive first order differences  $D_{30}(n, m)$  were calculated from each Mel spectrogram as follows:

$$D_{30}(n, m) = M_{log}^{30}(n, m) - M_{log}^{30}(n - 1, m) \quad (2)$$

The frame energy has also been included as a feature which resulted in a total of 54 features [22]. For extracting features from the audio we used the open-source toolkit OpenSMILE [23].

Finally, we used the Weka toolkit for feature evaluation with Information Gain (IG) feature evaluation and Correlation-based Feature Selection (CFS) to reduce the dimension of the feature space [24].

The IG feature evaluation is an univariate filter that calculates the worth of a feature by measuring the IG with respect to

the class [25], [26]. The output is a list of ranked features of which we selected best  $5n$  features, where  $n \in [1..10]$  and the whole feature set for comparison.

The CFS subset evaluation is a multivariate filter that seeks for subsets of features that are highly correlated with the class while having low intercorrelation [24], [25], [27]. We used BestFirst search algorithm in a forward search mode and a threshold of 5 non-improving nodes for consideration before terminating search. The CFS subset evaluation returned a list of 5 features.

### C. Classifier

In this work, we used a deep learning approach with initialized nets – LSTM and bi-directional LSTM (BLSTM) RNN architecture which in contrast to other RNNs does not suffer from the problem of vanishing gradients [28]. The BLSTM is a configuration of LSTM architecture that allows both forward and backward pass, which has been proven successful in many applications [8].

In addition, we evaluated different parameters, as the layout of LSTM and BLSTM hidden layers (54-30-54, 54-54-54, 156-256-156, 216-216-216, 216-316-216) and learning rates (1e-4, 1e-5, 1e-6). We used feed forward output layer with a logistic activation function and sum of squared error as objective function. The experiments were carried out with the CURRENNT toolkit [29].

## IV. RESULTS

Table II shows the evaluation results in an ascending order for the best 20 features that were selected with IG (IG-20), as described in §III-B and trained with LSTM-RNN. For every combination of parameters we conducted cross-validation on all three folds from Table I (six experiments) and computed an average UAR for results obtained from all speeds including vehicle stationary mode. The best result with an UAR of 93.2% was achieved with BLSTM network layout 216-216-216 and learning rate  $1e^{-5}$ .

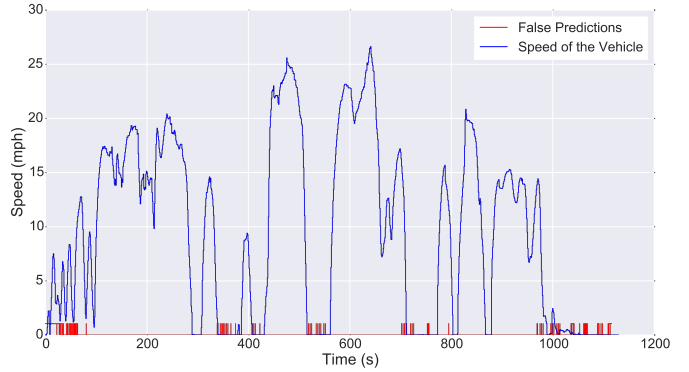
Additionally, we compared our results with the state-of-the-art approach of [5] that uses zero-norm minimization (L0) to select four most promising features (L0-4) from 125 ms audio bins of 1/3 octave bands (5000 Hz, 1600 Hz, 630 Hz and 200 Hz frequency bands). We trained SVMs with the Sequential Minimal Optimization (SMO) on our dataset and found a C parameter of  $1e^{-3}$  to give the best UAR of 67.4%. Furthermore, experiments with SVMs and IG-20 feature set were carried out and gave the best UAR of 78.8%.

Network	Feature set	C	UAR
SVM	Z0-4	$1e^{-3}$	67.4%
SVM	IG-20	$1e^{-3}$	78.8%
Network	Layout	LR	UAR
LSTM	216-216-216	$1e^{-4}$	66.3%
BLSTM	216-316-216	$1e^{-4}$	76.1%
LSTM	156-256-156	$1e^{-4}$	78.0%
LSTM	216-316-216	$1e^{-4}$	78.6%
BLSTM	54-54-54	$1e^{-4}$	79.4%
LSTM	54-30-54	$1e^{-4}$	79.5%
BLSTM	216-216-216	$1e^{-4}$	79.9%
LSTM	54-54-54	$1e^{-4}$	81.4%
BLSTM	156-256-156	$1e^{-4}$	82.9%
BLSTM	54-30-54	$1e^{-4}$	85.9%
BLSTM	54-30-54	$1e^{-5}$	86.1%
LSTM	216-316-216	$1e^{-6}$	88.6%
LSTM	54-30-54	$1e^{-5}$	88.6%
BLSTM	54-54-54	$1e^{-6}$	89.4%
LSTM	216-316-216	$1e^{-5}$	89.7%
BLSTM	216-316-216	$1e^{-6}$	89.8%
LSTM	54-30-54	$1e^{-6}$	89.8%
BLSTM	54-54-54	$1e^{-5}$	90.0%
BLSTM	156-256-156	$1e^{-6}$	90.1%
BLSTM	54-30-54	$1e^{-6}$	90.1%
LSTM	216-216-216	$1e^{-6}$	90.2%
LSTM	156-256-156	$1e^{-5}$	90.8%
BLSTM	216-216-216	$1e^{-6}$	91.0%
LSTM	156-256-156	$1e^{-6}$	91.1%
BLSTM	156-256-156	$1e^{-5}$	91.5%
LSTM	54-54-54	$1e^{-6}$	91.8%
LSTM	54-54-54	$1e^{-5}$	92.4%
BLSTM	216-316-216	$1e^{-5}$	92.6%
LSTM	216-216-216	$1e^{-5}$	92.6%
<b>BLSTM</b>	<b>216-216-216</b>	$1e^{-5}$	<b>93.2%</b>

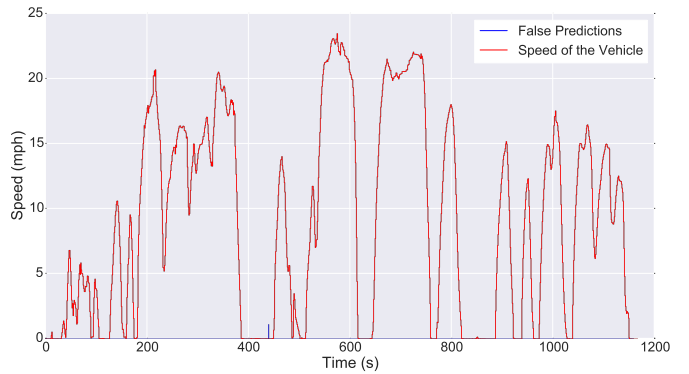
TABLE II: Comparison of state-of-the-art approach with SVMs and our approach with RNNs. The column LR is an abbreviation for Learning Rate.

Two out of three wet trips have significantly higher number of false predictions (1) at the beginning, where vehicle tires were dry before getting wetted from the surface, and (2) at the end of the trip, when the vehicle entered a parking lot with relatively dry road surface.

In Fig. 5 we compare speed and false predictions of wet and dry trips for the same route that has similar properties, which are described in §III-A. One can observe that all false predictions of wet trip 2 in Fig. 5a occurred below the speed of 2.9 mph, whilst Fig. 5b depicts a dry trip 2 and has only one false prediction when the vehicle is not moving. Therefore, discarding speeds below 2.9 mph improves the UAR to 100%. When we look only at speeds below 2.9 mph and ignore everything above we are still able to attain 74.5% UAR. The latter is possible only in presence of ambient sounds, as noises of vehicles that are driving by.



(a) An 18 min long wet trip showing speed and false predictions.



(b) A 19 min long dry trip showing speed and false predictions.

Fig. 5: Graphs for wet and dry road surfaces that clarify the correlation between low speed and inaccurate predictions.

## V. CONCLUSION

We proposed a deep learning approach based on LSTM-RNN for detecting road wetness from audio of the tire-surface interaction. This method is shown to be robust to vehicle speed, road type, and pavement quality on a dataset containing 785,826 bins of audio. It significantly outperforms the state-of-the-art SVMs and achieves an outstanding performance on the road wetness detection task with an 93.2% UAR for all vehicle speeds and 100% UAR for speeds above 2.9 mph. In future work, we will augment the feature set for estimating depth of water on the road surface and detecting hydroplaning conditions.

## ACKNOWLEDGMENT

Support for this work was provided by the New England University Transportation Center, and the Toyota Class Action Settlement Safety Research and Education Program. The views and conclusions being expressed are those of the authors, and have not been sponsored, approved, or endorsed by Toyota or plaintiffs' class counsel.

## REFERENCES

[1] Booz-Allen-Hamilton, "Ten-year averages from 2002 to 2012 based on nhtsa data," *US Department of Transportation - Federal Highway Administration*, 2012. [Online]. Available: [www.ops.fhwa.dot.gov/weather](http://www.ops.fhwa.dot.gov/weather)

[2] J. Andrey, B. Mills, M. Leahy, and J. Suggett, "Weather as a chronic hazard for road transportation in canadian cities," *Natural Hazards*, vol. 28, no. 2-3, pp. 319–343, 2003.

[3] J. Andrey, B. Mills, and J. Vandermolen, "Weather information and road safety," *Institute for Catastrophic Loss Reduction, Toronto, Ontario, Canada*, 2001.

[4] M. Mueller, "Sensor sensibility: Advanced driver assistance systems," *Vision Zero International*, 2015.

[5] J. Alonso, J. López, I. Pavón, M. Recuero, C. Asensio, G. Arcas, and A. Bravo, "On-board wet road surface identification using tyre/road noise and support vector machines," *Applied Acoustics*, vol. 76, pp. 407–415, 2014.

[6] A. Graves, M. Liwicki, S. Fernández, R. Bertolami, H. Bunke, and J. Schmidhuber, "A novel connectionist system for unconstrained handwriting recognition," *Pattern Analysis and Machine Intelligence, IEEE Transactions on*, vol. 31, no. 5, pp. 855–868, 2009.

[7] H. Mayer, F. Gomez, D. Wierstra, I. Nagy, A. Knoll, and J. Schmidhuber, "A system for robotic heart surgery that learns to tie knots using recurrent neural networks," *Advanced Robotics*, vol. 22, no. 13-14, pp. 1521–1537, 2008.

[8] A. Graves and J. Schmidhuber, "Framewise phoneme classification with bidirectional lstm and other neural network architectures," *Neural Networks*, vol. 18, no. 5, pp. 602–610, 2005.

[9] M. Wöllmer, F. Eyben, S. Reiter, B. Schuller, C. Cox, E. Douglas-Cowie, and R. Cowie, "Abandoning emotion classes-towards continuous emotion recognition with modelling of long-range dependencies." in *INTERSPEECH*, vol. 2008, 2008, pp. 597–600.

[10] F. Weninger and B. Schuller, "Audio recognition in the wild: Static and dynamic classification on a real-world database of animal vocalizations," in *acoustics, speech and signal processing (ICASSP), 2011 IEEE international conference on*. IEEE, 2011, pp. 337–340.

[11] D. Eck and J. Schmidhuber, "Finding temporal structure in music: Blues improvisation with lstm recurrent networks," in *Neural Networks for Signal Processing, 2002. Proceedings of the 2002 12th IEEE Workshop on*. IEEE, 2002, pp. 747–756.

[12] Y. Horita, S. Kawai, T. Furukane, and K. Shibata, "Efficient distinction of road surface conditions using surveillance camera images in night time," in *Image Processing (ICIP), 2012 19th IEEE International Conference on*. IEEE, 2012, pp. 485–488.

[13] M. Yamada, T. Oshima, K. Ueda, I. Horiba, and S. Yamamoto, "A study of the road surface condition detection technique for deployment on a vehicle," *JSAE review*, vol. 24, no. 2, pp. 183–188, 2003.

[14] M. Jokela, M. Kutila, and L. Le, "Road condition monitoring system based on a stereo camera," in *Intelligent Computer Communication and Processing, 2009. ICCP 2009. IEEE 5th International Conference on*. IEEE, 2009, pp. 423–428.

[15] M. Amthor, B. Hartmann, and J. Denzler, "Road condition estimation based on spatio-temporal reflection models," pp. 3–15, 2015.

[16] V. V. Viikari, T. Varpula, and M. Kantanen, "Road-condition recognition using 24-ghz automotive radar," *Intelligent Transportation Systems, IEEE Transactions on*, vol. 10, no. 4, pp. 639–648, 2009.

[17] K. Iwao and I. Yamazaki, "A study on the mechanism of tire/road noise," *JSAE review*, vol. 17, no. 2, pp. 139–144, 1996.

[18] R. Birken, G. Schirner, and M. Wang, "Voters: design of a mobile multi-modal multi-sensor system," in *Proceedings of the Sixth International Workshop on Knowledge Discovery from Sensor Data*. ACM, 2012, pp. 8–15.

[19] L. Fridman, D. E. Brown, W. Angell, I. Abdić, B. Reimer, and H. Y. Noh, "Automated synchronization of driving data using vibration and steering events," *arXiv preprint arXiv:1510.06113*, 2015.

[20] W. D. Paterson, "International roughness index: Relationship to other measures of roughness and riding quality," *Transportation Research Record*, no. 1084, 1986.

[21] MassDOT, "Road inventory - massdot planning," 2015. [Online]. Available: <https://www.massdot.state.ma.us/planning/Main/MapsDataandReports/Data/GISData/RoadInventory.aspx>

[22] E. Marchi, F. Vesperini, F. Weninger, F. Eyben, S. Squartini, and B. Schuller, "Non-linear prediction with lstm recurrent neural networks for acoustic novelty detection," in *Neural Networks (IJCNN), 2015 International Joint Conference on*. IEEE, 2015, pp. 1–7.

[23] F. Eyben, F. Weninger, F. Gross, and B. Schuller, "Recent developments in opensmile, the munich open-source multimedia feature extractor," in *Proceedings of the 21st ACM international conference on Multimedia*. ACM, 2013, pp. 835–838.

[24] M. Hall, E. Frank, G. Holmes, B. Pfahringer, P. Reutemann, and I. H. Witten, "The weka data mining software: an update," *ACM SIGKDD explorations newsletter*, vol. 11, no. 1, pp. 10–18, 2009.

[25] A. G. Kargowda, A. Manjunath, and M. Jayaram, "Comparative study of attribute selection using gain ratio and correlation based feature selection," *International Journal of Information Technology and Knowledge Management*, vol. 2, no. 2, pp. 271–277, 2010.

[26] M. Hall, G. Holmes *et al.*, "Benchmarking attribute selection techniques for discrete class data mining," *Knowledge and Data Engineering, IEEE Transactions on*, vol. 15, no. 6, pp. 1437–1447, 2003.

[27] M. A. Hall, "Correlation-based feature subset selection for machine learning," Ph.D. dissertation, University of Waikato, Hamilton, New Zealand, 1998.

[28] S. Hochreiter and J. Schmidhuber, "Long short-term memory," *Neural computation*, vol. 9, no. 8, pp. 1735–1780, 1997.

[29] J. Weninger, Felix Bergmann and B. Schuller, "Introducing currennt - the munich open-source cuda recurrent neural network toolkit," *Journal of Machine Learning Research*, no. 16, pp. 547–551, 2014.